Support Information

Self-Activated $LiGa_5O_8$ storage phosphor: The insights into photo/thermo/mechano-stimulated NIR luminescence

Min Jia,[a] Xiangyu Zhang,*[b] Xue Yang,[a] Zehao Lin,[a] Dingjun Jia,[a] Yuqiang Wang,[a] Sining Yun,[c] and Dangli Gao*[a]

[a] College of Science, Xi'an University of Architecture and Technology, Xi'an, Shaanxi 710055, China

[b] Functional Materials Laboratory (FML), School of Materials Science and Engineering, Xi'an University of Architecture and Technology, Xi'an 710055, China

[c] Department of Physics, Georgia Southern University, Statesboro, GA 30460, USA

*Corresponding Author

E-mail addresses: xyzhang@chd.edu.cn (X. Zhang), gaodangli@163.com, gaodangli@xauat.edu.cn (D. Gao).

Supporting Information contains:

- The relative enthalpies (eV) of $LiGa_5O_8$ with O_i, $V_O^{\bullet\bullet}$ and V_{Li}'.
- Three-dimensional plots and 2D representation of Young's moduli, Shear moduli and Poisson ratio for LGO.
- The maximum and minimum elastic modulus and their ratio of LGO with a $V_O^{\bullet\bullet}$ (recorded as $V_O^{\bullet\bullet}$ model), LGO with a O_i'' (recorded as O_i'' model), and LGO with a V_{Li} (recorded as V_{Li}' model), with perfect LGO as reference (recorded as LGO model).
- The electronic band structures and PDOS of LGO.
- Differential charge density of LGO with O_i model.
- Characterization of stability of LGO under stress loading through phonon spectra. Phonon spectra at 8% and 6% uniaxial strains along the *x* direction (a, b), *y* direction (c, d) and *z* direction (e, f).
- Changes in energy bands and PDOS of LGO with O_i'' under uniaxial strain.
- PersL decay curves of 254 nm pre-charged LGO.
- The flexible thin films composed by PDMS and LGO phosphor.

Table S1. The relative enthalpies (eV) of $LiGa_5O_8$ with O_i, $V_O^{\bullet\bullet}$ and V_{Li}'.

Name	Enthalpy	Relative Enthalpy
$Li1O_5$	-56262.64	433.18
$Ga1O_5$	-56262.45	432.99
$Ga2O_3$	-56262.47	433.01
O_i	-55391.04	871.41
V_{Li}'	-55197.55	1064.9
LGO	-56262.45	0

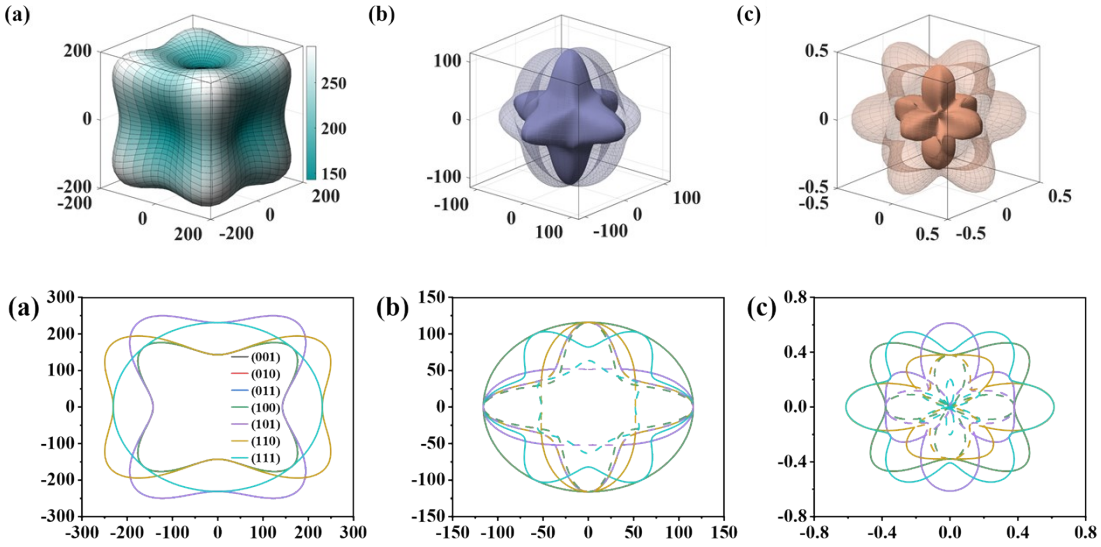

Figure S1. Three-dimensional plots and 2D representation of Young's moduli, Shear moduli and Poisson ratio for LGO.

Table S2. The maximum and minimum elastic modulus and their ratio of LGO with a $V_O^{\bullet\bullet}$ (recorded as $V_O^{\bullet\bullet}$ model), LGO with a O_i'' (recorded as O_i'' model), and LGO with a V_{Li} (recorded as V_{Li}' model), with perfect LGO as reference (recorded as LGO model).

		E_{max}	E_{min}	ratio	G_{max}	G_{min}	ratio	v_{max}	v_{min}	ratio
$V_O^{\bullet\bullet}$	(100)	205.54	121.21	1.70	107.27	44.36	2.42	0.55	0.03	18.33
	(010)	206.28	121.20	1.70	107.30	46.69	2.30	0.59	0.04	14.75
	(001)	200.94	123.56	1.63	107.28	48.10	2.23	0.60	0.04	15.00
	(011)	254.31	132.23	1.92	106.58	44.36	2.40	0.55	0.03	18.33
	(101)	254.23	123.58	2.06	105.82	46.49	2.28	0.57	0.04	14.25
	(110)	251.92	121.22	1.08	107.30	48.10	2.23	0.57	0.04	14.25
	(111)	206.04	194.42	1.06	104.75	44.36	2.36	0.57	0.04	14.25
	All	260.88	121.22	2.15	107.26	44.39	2.42	0.60	0.03	20.00
O_i''	(100)	209.95	129.07	1.63	109.83	47.77	2.30	0.58	0.02	29.00
	(010)	210.20	129.07	1.63	109.84	48.06	2.29	0.58	0.03	19.33
	(001)	221.04	131.08	1.69	109.79	48.06	2.28	0.59	0.03	19.67
	(011)	268.11	131.40	2.04	109.79	47.79	2.30	0.58	0.02	29.00
	(101)	262.66	131.06	2.00	109.79	48.08	2.28	0.58	0.03	19.33
	(110)	268.12	129.02	2.08	107.96	48.05	2.24	0.59	0.03	19.67
	(111)	221.39	206.06	1.07	108.95	47.77	2.28	0.59	0.03	19.67
	All	267.60	129.12	2.07	109.84	47.77	2.30	0.59	0.03	19.67
V_{Li}'	(100)	188.07	105.95	1.78	100.06	39.33	2.54	0.61	0.04	15.25
	(010)	187.71	109.56	1.71	99.81	42.12	2.37	0.65	0.08	8.13
	(001)	184.89	105.96	1.74	100.04	38.69	2.59	0.60	0.04	15.00
	(011)	237.22	109.59	2.16	99.81	39.32	2.54	0.61	0.04	15.25
	(101)	239.89	105.95	2.26	97.14	42.13	2.31	0.65	0.08	8.13
	(110)	239.86	113.28	2.12	100.06	38.67	2.59	0.60	0.04	15.00
	(111)	190.56	178.05	1.07	96.25	38.69	2.48	0.65	0.08	8.13
	All	239.63	106.55	2.25	100.03	38.67	2.59	0.65	0.04	16.25
LGO	(100)	230.91	142.88	1.62	115.85	51.80	2.24	0.61	0.003	20.33
	(010)	230.91	142.88	1.62	115.85	51.80	2.24	0.61	0.003	20.33
	(001)	230.91	142.88	1.62	115.85	51.80	2.24	0.61	0.003	20.33
	(011)	290.60	142.88	2.03	115.85	51.80	2.24	0.61	0.003	20.33
	(101)	290.60	142.88	2.03	115.85	51.80	2.24	0.61	0.003	20.33
	(110)	290.60	142.88	2.03	115.85	51.80	2.24	0.61	0.003	20.33
	(111)	230.91	230.91	1.00	115.85	51.80	2.24	0.61	0.003	20.33
	All	290.12	142.88	2.03	115.85	51.83	2.24	0.61	0.003	20.33

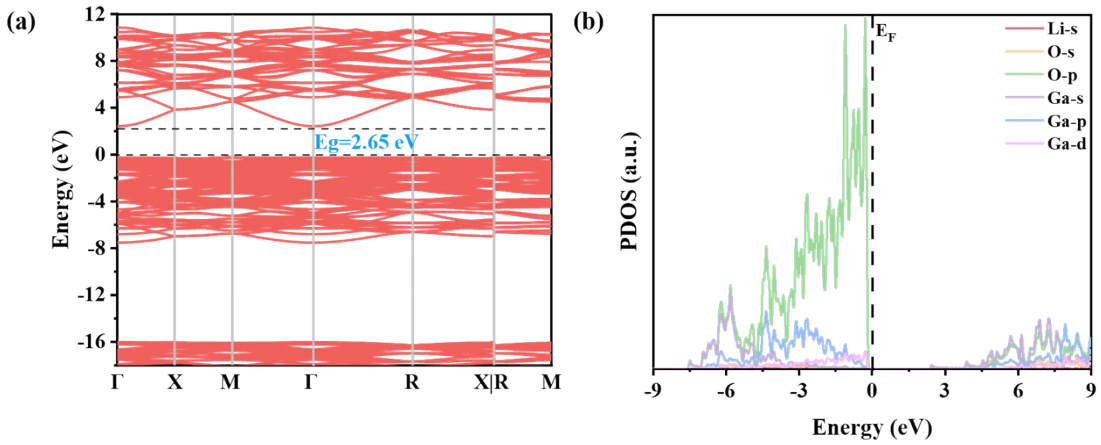

Figure S2. The electronic band structures and PDOS of LGO.

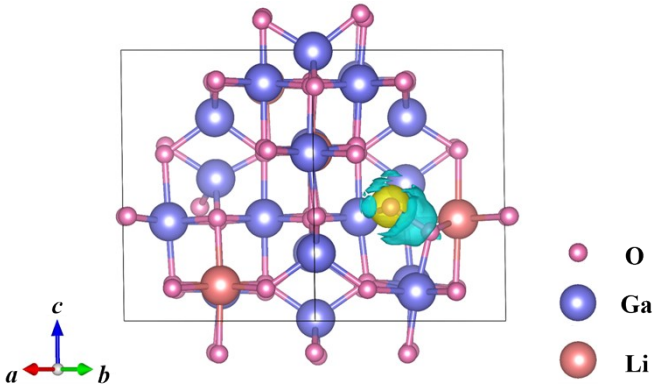

Figure S3. Differential charge density of LGO with O_i model.

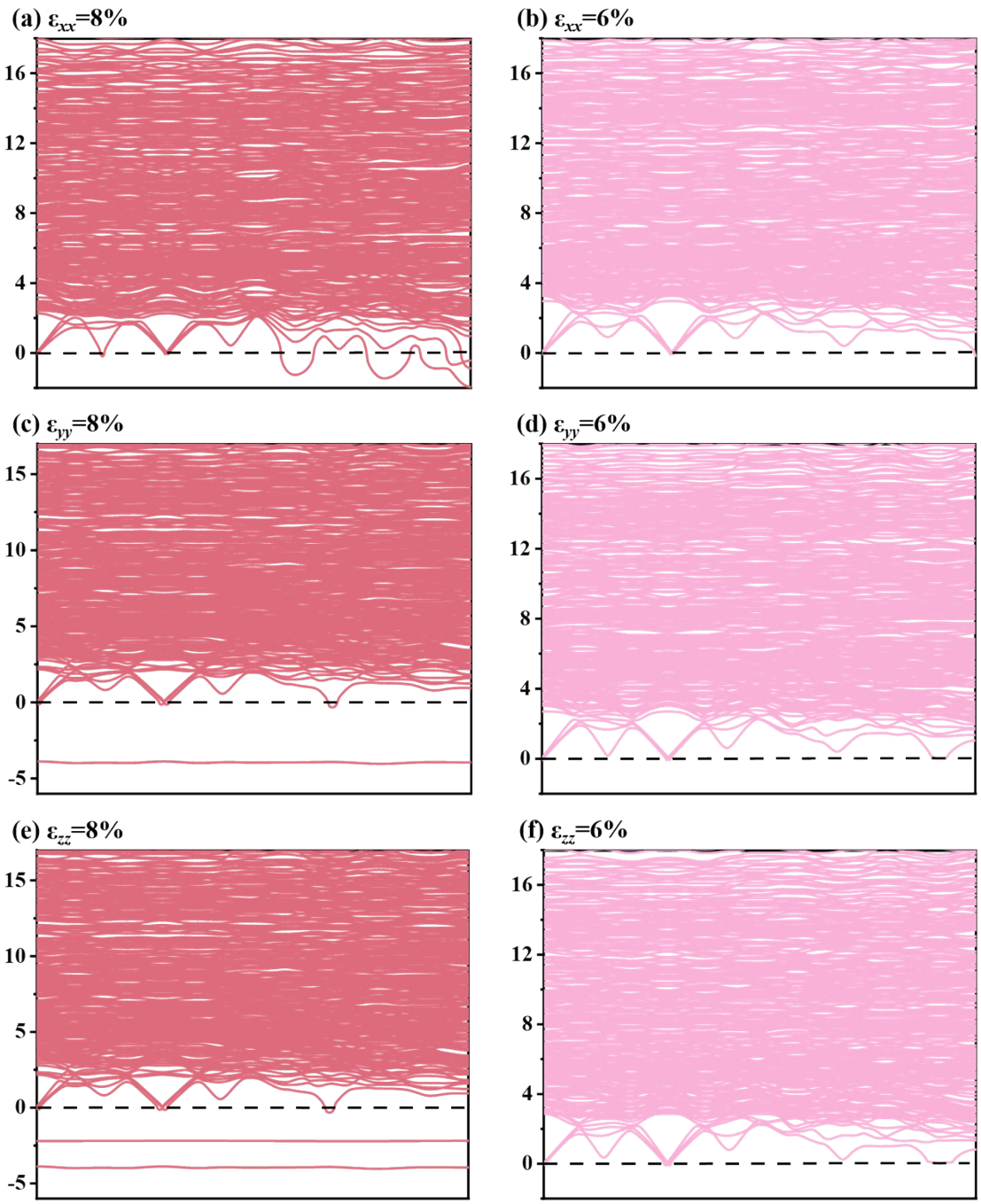

Figure S4. Characterization of stability of LGO under stress loading through phonon spectra. Phonon spectra at 8% and 6% uniaxial strains along the *x* direction (a, b), *y* direction (c, d) and *z* direction (e, f).

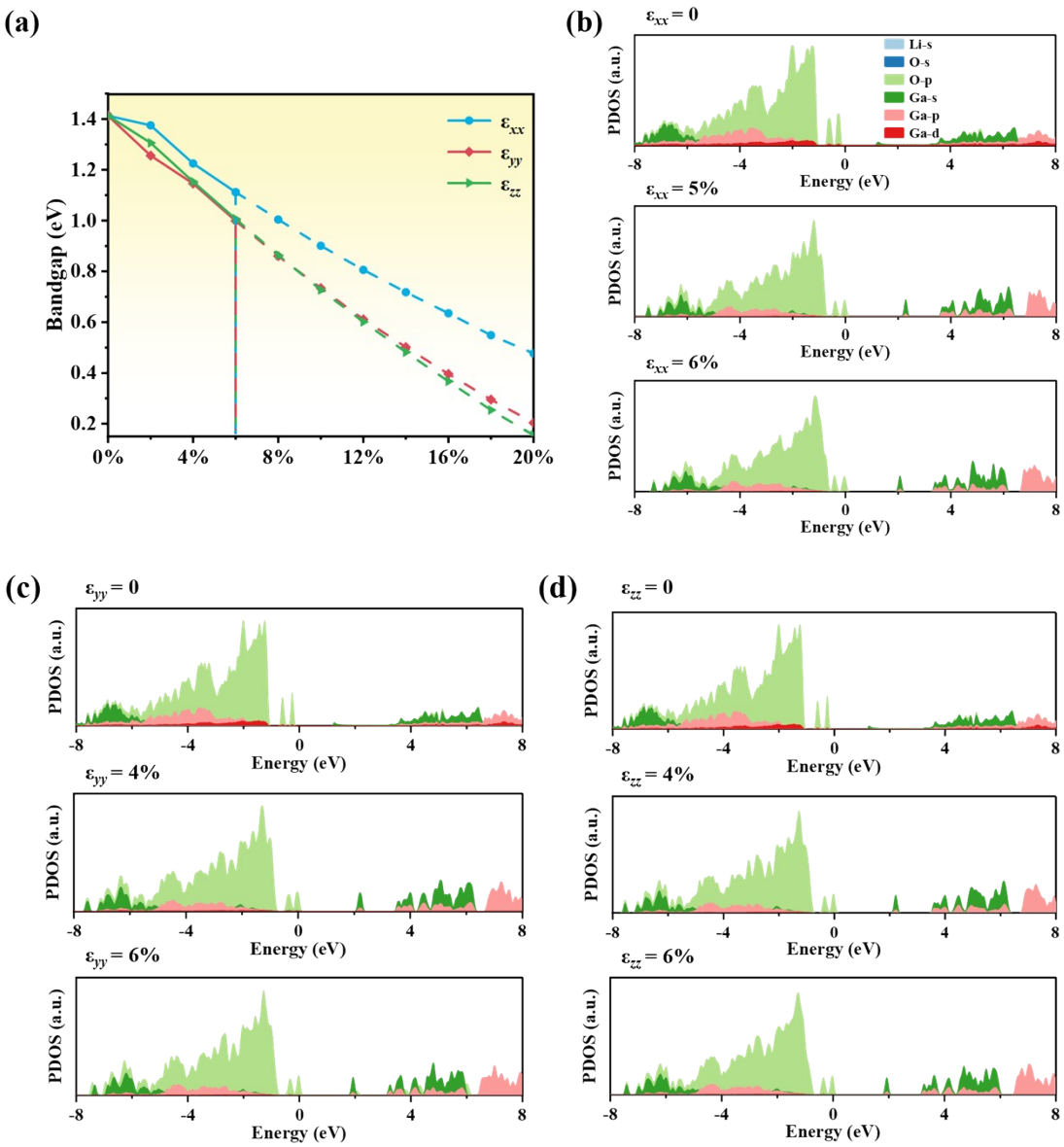

Figure S5. Changes in energy bands and PDOS of LGO with O_i'' under uniaxial strain.

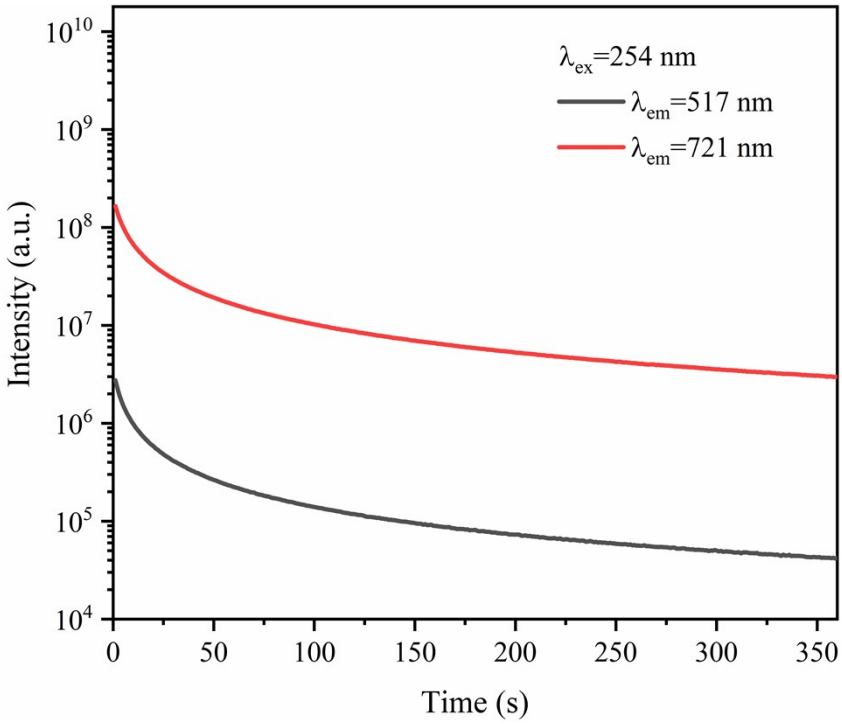

Figure S6. PersL decay curves of 254 nm pre-charged LGO.

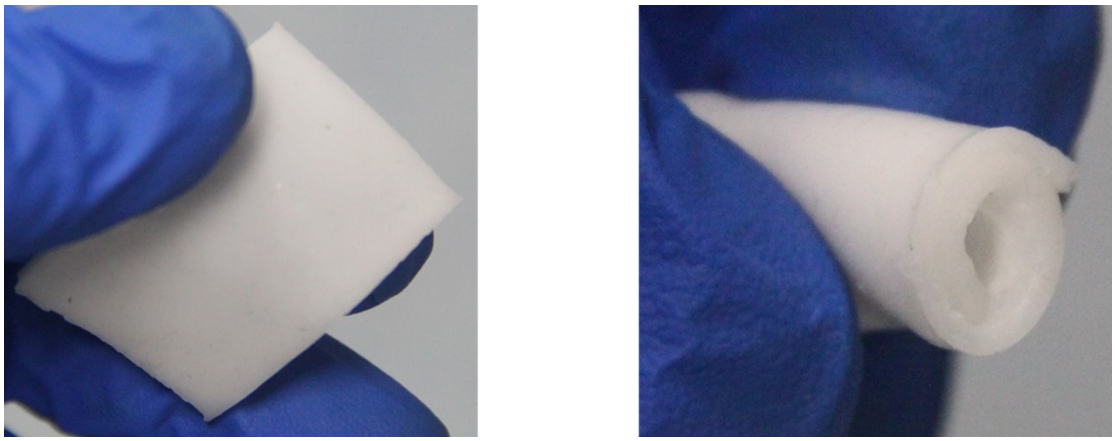

Figure S7. The flexible thin films composed by PDMS and LGO phosphor.